

## Enhanced magnetic moment in Fe-doped Pd<sub>n</sub> clusters ( $n = 1-13$ ): a density functional study

This article has been downloaded from IOPscience. Please scroll down to see the full text article.

2009 J. Phys.: Condens. Matter 21 396001

(<http://iopscience.iop.org/0953-8984/21/39/396001>)

View [the table of contents for this issue](#), or go to the [journal homepage](#) for more

Download details:

IP Address: 129.252.86.83

The article was downloaded on 30/05/2010 at 05:28

Please note that [terms and conditions apply](#).

# Enhanced magnetic moment in Fe-doped $\text{Pd}_n$ clusters ( $n = 1-13$ ): a density functional study

Sonali Barman<sup>1</sup>, D G Kanhere<sup>2</sup> and G P Das<sup>1</sup>

<sup>1</sup> Department of Materials Science, Indian Association for the Cultivation of Science, Kolkata 700032, India

<sup>2</sup> Department of Physics, University of Pune, Pune 411 007, India

Received 10 March 2009, in final form 7 July 2009

Published 1 September 2009

Online at [stacks.iop.org/JPhysCM/21/396001](http://stacks.iop.org/JPhysCM/21/396001)

## Abstract

Here we report a systematic theoretical study of the equilibrium structures, electronic and magnetic properties of  $\text{FePd}_{n-1}$  clusters with  $n = 1-13$ , within the framework of density functional theory. The results show that the doping of a single Fe impurity enhances the binding energies as well as the magnetic moment of the  $\text{Pd}_n$  clusters. Interestingly, in the mid-size region ( $n = 5-7$ ), Fe substitution in  $\text{Pd}_n$  clusters results in a three fold enhancement in the magnetic moment. We find that the geometries of the host clusters do not change significantly after the addition of an Fe atom, except for  $n = 6, 7, 11, 12$ . In the lowest energy configurations, the Fe atom tries to increase its coordination number by moving from the convex to the interior site as the number of Pd atoms varies from 2 to 12.

(Some figures in this article are in colour only in the electronic version)

## 1. Introduction

It is a matter of current interest to look into the properties of clusters which are neither atomic-like nor extended solid-like. For example, Pd has no magnetic property either in the atomic state or in the bulk phase, but small Pd clusters, which are considered as an intermediate phase between the former two phases, exhibit magnetic behavior. In homogeneous clusters the physical and chemical properties can be tailored, simply by varying the size of the cluster. An additional degree of freedom comes into play for tuning the material property if other elemental atoms are doped in the host cluster. Such bimetallic clusters have attracted considerable attention due to their unique structural, electronic, magnetic, optical, and catalytic properties compared to mono-atomic clusters [1–10].

Conflicting results have been reported in the literature regarding the magnetism of pure Pd clusters. Stern–Gerlach deflection experiments [11] could not find any magnetic moment in Pd clusters in the temperature range 60 K and above, while photoemission studies [12] reported a Ni-like magnetic behavior for  $\text{Pd}_n$  with  $n = 3-6$  and a non-magnetic Pt-like behavior for  $n > 15$ . Another experimental study reported that, in the case of large Pd clusters (50–70 Å) each surface atom exhibits a  $(0.23 \pm 0.19) \mu_B$  magnetic

moment [13]. Moseler *et al* [14] carried out spin-density-functional calculations on small  $\text{Pd}_n$  ( $n = 2-7, 13$ ) clusters and observed a finite size magnetic moment. The atomic, electronic and magnetic properties of pure  $\text{Pd}_n$  clusters ( $n = 2-23, 55, 147$ ) have been carried out by Kumar *et al* [15] using the ultrasoft pseudopotential plane wave method with a spin-polarized GGA approximation. They reported an icosahedral growth in these clusters, and a size-dependent oscillatory magnetic moment that is not confined to the surface atoms alone. First principles calculations by Lee *et al* [16] reported that  $\text{Pd}_{15}$  and  $\text{Pd}_{19}$  clusters having cubic symmetry exhibit  $0.53 \mu_B$  and  $0.32 \mu_B$  moments, respectively, per Pd atom.

In this work, we report the first principles investigation of the structural and magnetic properties of bimetallic  $\text{FePd}_{n-1}$  ( $n = 1-13$ ) clusters, where we mainly focus on two major issues: one is to outline how the magnetic property depends on cluster size, while the other is to investigate how the magnetic moment gets perturbed when a single Fe impurity is doped into the Pd host cluster. Such investigations are important as they provide a powerful tool to gain insights into the physical and chemical properties of the doped system as a function of size. In the bulk phase both Fe and Pd acquire different physical properties. It is well known that Fe is a ferromagnetic material, while Pd, like all 4d elements, is non-magnetic in the

bulk phase, nearly satisfies the Stoner criterion and has a high paramagnetic susceptibility. However a 6% enhancement in the lattice constant induces a paramagnetic to ferromagnetic transition in the bulk phase [17–19]. In addition, a very interesting local moment system has been observed when a 3d impurity (Fe, Co or Ni) is embedded in the Pd matrix thus inducing a large host polarization [20, 21]. In particular, the introduction of an Fe impurity into bulk Pd results in a giant magnetic moment, where the large atomic moment of Fe ( $3.47 \mu_B$ ) is maintained with a ferromagnetic polarization of the surrounding Pd atoms. In the past few decades, many experimental as well as theoretical investigations have been carried out in order to analyze the magnetic properties of Fe–Pd compounds in the form of bulk alloys [22, 23], thin films [24, 25] and multilayered structures [26].

However, to the best of our knowledge, much less attention has been given to the magnetism of Fe–Pd heteroatomic clusters or nanoparticles. From the experimental point of view, recent reports have shown that a wide variety of Fe–Pd nanoparticles with different sizes, morphologies and compositions can be synthesized [27–31]. The experimental characterization of these systems reveals the dependence of the saturation magnetization on particle size and composition. The magnetic behavior of FePd nanoparticles ( $N =$  up to 561) [32] has been theoretically investigated as a function of particle size, surface structure and impurity concentration. Other theoretical studies, using local spin density functional theory and molecular cluster models, reported that a single Fe impurity in relatively small Pd clusters ( $n = 55$  and 13) [33–35] results in a large induced magnetic moment in the host Pd metal due to the strong hybridization of the Fe 3d and Pd 4d states whereas, a local moment  $\sim 3.2 \mu_B$  is maintained at the Fe site, which is a signature of bulk materials.

The recent experimental investigation of an isolated Fe impurity in  $\text{Pd}_{0.95}\text{M}_{0.05}$  alloys ( $M = \text{Ni, Rh, Mo, Ag, Cd, In, Sn, Th}$  and  $\text{U}$ ), using the time differential perturbed angular distribution (TDPAD) technique shows a strong spin polarization associated with the Pd 4d band electrons, and, depending on the element  $M$  added to the Pd matrix, a strong enhancement or suppression of the ferromagnetic host spin polarization associated with the giant moment of Fe was observed [36]. A detailed first principles investigation of the local magnetic response of isolated Fe in dilute  $\text{Pd}_{1-x}\text{V}_x$  with increasing  $V$  concentration has been carried out [37], in order to understand the spin-fluctuation behavior and the effect of the hyperfine field in Pd–V alloys. The large magnetic moment of Fe is found to be suppressed by introducing  $V$  into Pd matrix, through a charge transfer process. The hyperfine field calculated at the Fe nucleus shows that the process reduces the negative magnetic field contributed from the core  $s$  levels, while it enhances the positive contribution of the valence  $4s$  level to the magnetic field, leading to an overall less negative hyperfine field at the nucleus.

Motivated by these results, in this paper, we have investigated the structural evaluation, bonding characters and magnetic properties of  $\text{FePd}_n$  ( $n = 1$ –12) clusters. The paper is organized as follows. In section 2 we present the details of the computational method. In section 3 we present the

calculated results and corresponding discussions, and the main conclusions are given in section 4.

## 2. Computational details

The impurity atom can interact with the host cluster in three possible ways, namely, (a) the impurity atom can occupy the center of the cage formed by the host cluster (endohedral), (b) the impurity atom can be adsorbed on the surface of the host cluster (exohedral) and (c) the impurity atom can replace one atom from the host cluster (substitutional). Based on this approach we have generated a large number of initial structures (at least 20 with cluster size  $n > 7$ ) for each size ( $n = 2$ –13) of  $\text{FePd}_{n-1}$  clusters to explore the lowest energy configuration. To get the exact ground-state magnetic moment we have explicitly considered all possible spin configurations for each geometrical structure. The geometry optimizations are carried out using density functional theory (DFT) with the projector augmented wave (PAW) pseudopotential method [38, 39]. For spin-polarized gradient correction (GGA) we have used the Perdew–Burke–Ernzerhof exchange correlation functional [40] as implemented in the Vienna *ab initio* simulation package (VASP) [41]. For the Fe atom  $3d^75s^1$  electrons are treated as valance electrons with those for the Pd atom being  $4d^{10}5s^0$ .  $\Gamma$ -point calculations have been performed by expanding the wavefunction in a plane wave basis set with a kinetic energy cut off at 400 eV. In the geometry and spin optimization all the structural parameters are fully optimized without any symmetry constraints using conjugate and quasi-Newtonian methods until all the force components are less than a threshold value  $0.005 \text{ eV \AA}^{-1}$ . Simple cubic supercells are used with periodic boundary conditions where the neighboring clusters are kept separated by at least a distance of  $10 \text{ \AA}$  vacuum space.

## 3. Results and discussion



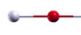




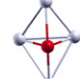





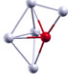

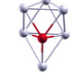

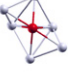


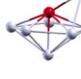
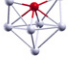
### 3.1. Structural details

In this section we discuss the evolutionary trend of the lowest energy structures of the  $\text{FePd}_{n-1}$  clusters ( $n = 1$ –13) along with some low-lying isomers as shown in figures 1 and 2. The ground-state configurations of pure  $\text{Pd}_n$  clusters are also shown for comparison. Before beginning our discussions, we would like to mention that the ionic radii of Pd and Fe atoms are  $0.86 \text{ \AA}$  and  $0.65 \text{ \AA}$  respectively, and the electronegativity of Pd(2.20) is larger than that of Fe(1.83).

The binding energy per atom (BE) of a cluster is defined as the energy gain in assembling the cluster from its isolated constituent atoms. Hence the BE of  $\text{FePd}_{n-1}$  cluster is


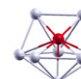
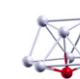
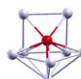


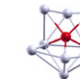
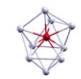
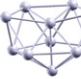
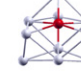
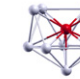
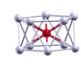
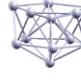
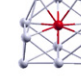
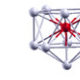
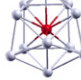

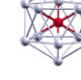
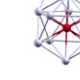
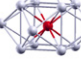
$$\text{BE} = -[E(\text{FePd}_{n-1}) - (n-1)E(\text{Pd}) - E(\text{Fe})]/n. \quad (1)$$

The FePd dimer has a much higher BE ( $1.33 \text{ eV/atom}$ ) and a much shorter bond length ( $2.2 \text{ \AA}$ ) as compared to those of a pure  $\text{Pd}_2$  dimer ( $\text{BE} = 0.65 \text{ eV/atom}$  and  $\text{Pd–Pd}$  bond length =  $2.5 \text{ \AA}$ ). The magnetic moment of the Fe–Pd dimer is  $4 \mu_B$ , which is the same as the magnetic moment of the Fe atom.

n	Pd <sub>n</sub>	FePd <sub>n-1</sub> ; (n = 3 - 8)	
3		 	$\Delta E(\text{eV})=0.00$ Mag. mom. ( $\mu_B$ ) = 2 0.68
4		 	$\Delta E(\text{eV})=0.00$ Mag. mom. ( $\mu_B$ ) = 4 0.24
5		  	$\Delta E(\text{eV})=0.00$ Mag. mom. ( $\mu_B$ ) = 6 0.32    0.37
6		  	$\Delta E(\text{eV})=0.00$ Mag. mom. ( $\mu_B$ ) = 6 0.15    0.24
7		  	$\Delta E(\text{eV})=0.00$ Mag. mom. ( $\mu_B$ ) = 6 0.0003    0.004
8		  	$\Delta E(\text{eV})=0.00$ Mag. mom. ( $\mu_B$ ) = 6 0.11    0.23

**Figure 1.** The ground-state geometries of Pd<sub>n</sub> clusters (column 2). The structures on right side show the lowest energy structure (column 3) and some of the low-lying configurations for FePd<sub>n-1</sub> clusters (n = 3–8). n (column 1) represents the total number of atoms in the respective clusters. The dark sphere represents the Fe atom and the lightly shaded spheres represent the Pd atoms.

The BE increases to 1.72 eV/atom for the isosceles triangular FePd<sub>2</sub> cluster, where the Fe–Pd distance is 2.3 Å and the Pd–Pd bond length is 2.7 Å. The magnetic moment of FePd<sub>2</sub> is 4 μ<sub>B</sub>. A linear chain isomer, as shown in figure 1, is found to be 0.68 eV higher in energy compared to this ground-state structure. Both in homo- and hetero-atomic clusters the transition from a planar to a three dimensional motif occurs at n = 4 onwards. In line with pure Pd<sub>4</sub>, the lowest energy structure of the FePd<sub>3</sub> cluster adopts a tetrahedral configuration. The BE is 1.92 eV/atom and the magnetic moment of this cluster is 4 μ<sub>B</sub>. In this configuration the Fe–Pd and Pd–Pd bond lengths are 2.4 Å and 2.7 Å respectively. A planar Fe-centered rhombus structure is one of the low-lying isomers at a slightly higher energy (0.24 eV). The FePd<sub>4</sub> configuration favors the trigonal bipyramidal (TBP) configuration as its lowest energy state and to maximize its

n	Pd <sub>n</sub>	FePd <sub>n-1</sub> ; (n = 9 - 13)		
9		  	$\Delta E(\text{eV})=0.00$ Mag. mom. ( $\mu_B$ ) = 8 0.09    0.22	
10		  	$\Delta E(\text{eV})=0.00$ Mag. mom. ( $\mu_B$ ) = 8 0.06    0.10	
11		  	$\Delta E(\text{eV})=0.00$ Mag. mom. ( $\mu_B$ ) = 8 0.11    0.13	
12		  	$\Delta E(\text{eV})=0.00$ Mag. mom. ( $\mu_B$ ) = 8 0.06    0.39	
13		  	$\Delta E(\text{eV})=0.00$ Mag. mom. ( $\mu_B$ ) = 10 0.63    0.65  0.79    1.9	

**Figure 2.** The ground-state geometries of Pd<sub>n</sub> clusters (column 2). The structures on right side show the lowest energy structure (column 3) and some of the low-lying configurations for FePd<sub>n-1</sub> clusters (n = 9–13). n (column 1) represents the total number of atoms in the respective clusters. The dark sphere represents the Fe atom and the lightly shaded spheres represent the Pd atoms.

coordination number, Fe substitutes one host atom from one corner of the triangular base. The BE and the magnetic moment of this cluster are 2.08 eV/atom and 6 μ<sub>B</sub> respectively. The Fe–Pd bond length in the triangular base is 2.4 Å and that from apex to the base atom is 2.3 Å, while the Pd–Pd bond length is much longer (2.8 Å). A square pyramidal and another TBP structure with an Fe atom at the vertex (coordination of Fe is 3) are found as two low-lying isomers with only 0.32 eV and 0.37 eV higher in energy respectively compared to the ground-state structure.

Pure Pd<sub>6</sub> and Pd<sub>7</sub> clusters are found to prefer an octahedral motif and a pentagonal bipyramidal (PBP) motif respectively as the lowest energy isomers. However, the substitution of Fe in these clusters leads to a different ground-state configuration. The FePd<sub>5</sub> cluster favors a capped TBP isomer, with a BE of 2.18 eV/atom, which is obtained by capping a Pd atom

on the ground-state geometry of the  $\text{FePd}_4$  cluster. In this configuration, the shortest Fe–Pd distance is 2.4 Å and the bond lengths between the Pd atoms vary from 2.7 to 2.8 Å. An edge capped TBP structure and octahedron motif, with Fe atoms at the vertex, are the other low-lying isomers with energies higher by 0.15 eV and 0.2 eV respectively.

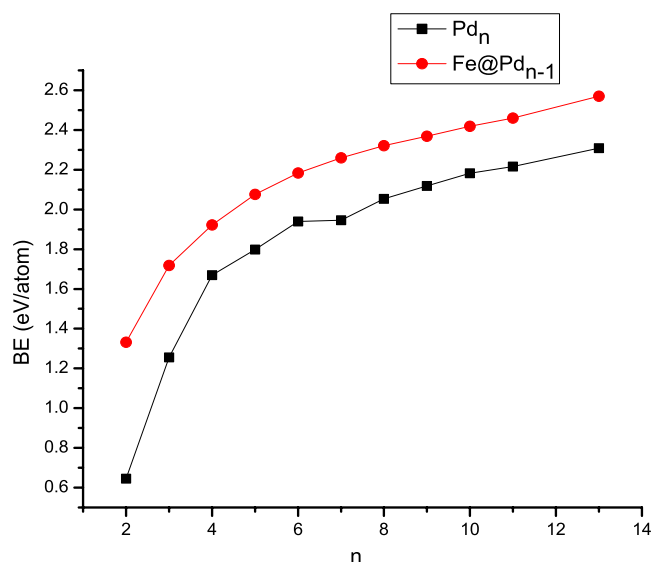
For the case of doped the  $\text{FePd}_6$  cluster, a TBP structure capped with two Pd atoms on the same side of the triangular base turns out to be lowest energy configuration. The BE and the magnetic moment of this configuration are 2.26 eV and  $6 \mu_B$  respectively. The shortest Fe–Pd bond length is 2.4 Å and that between the Pd atoms vary from 2.7 to 2.8 Å as in the  $\text{FePd}_5$  cluster. Two nearly degenerate structures (capped octahedron and a bi-capped TBP) are found to compete with the ground-state configuration. A PBP motif (not shown) with an Fe atom at the vertex site is found as a higher energy isomer ( $\Delta E = 0.04$  eV). This configuration is important as it ultimately leads to an icosahedron geometry as the cluster size grows.

Both  $\text{Pd}_8$  and  $\text{FePd}_7$  clusters adopt a bi-capped octahedron structure as their ground state, where in the doped cluster the Fe atom goes to one of the substitutional sites such that maximum coordination is achieved. The BE of this cluster increases to 2.32 eV and the magnetic moment is  $6 \mu_B$ . In this structure, the Fe–Pd bond lengths vary from 2.4 to 2.6 Å and that between the Pd atoms vary from 2.7 to 2.9 Å. Two other higher energy isomers are also found.

A bi-capped pentagonal bipyramidal (PBP) structure with  $\text{BE} = 2.37$  eV and magnetic moment of  $8 \mu_B$  is found as a lowest energy structure for a  $\text{FePd}_8$  cluster. The Fe–Pd bond length is 2.5 Å and the average Pd–Pd bond length is 2.7 Å. A similar structure with an Fe atom at the lower vertex is found as a meta-stable isomer with 0.087 eV higher in energy compared to the ground state structure.

This trend of capping continues with the addition of another Pd atom, thus a tri-capped PBP structure with an Fe atom at the vertex of PBP, similar to the ground-state geometry of a pure  $\text{Pd}_{10}$  cluster is found as the lowest energy structure of  $\text{FePd}_9$  cluster. The BE of this configuration is 4.2 eV and the corresponding magnetic moment is  $8 \mu_B$ . The Fe–Pd bond lengths vary from 2.5 to 2.7 Å and those between Pd–Pd vary from 2.6 to 2.8 Å. Other low-lying isomers are shown in figure 2.

Pure  $\text{Pd}_n$  clusters with  $n = 10$ –12 prefer the icosahedron structure as their ground state. But due to the substitution of Fe in the  $\text{Pd}_{10}$  host cluster, the doped cluster adopts a different geometry. The structure is like three interlinked octahedra with an Fe atom serving as the common vertex. The BE and magnetic moment of this lowest energy configuration are 2.46 eV and  $8 \mu_B$  respectively. An icosahedron structure with an Fe atom at the vertex of the PBP is found as a low-lying isomer with 0.11 eV higher in energy compared to the lowest structure. A pentagonal prism cage structure with an Fe atom encapsulated at the interior site (10 nearest neighbor P atoms) turns out to be another higher energy isomer. The magnetic moment of this configuration is  $6 \mu_B$ . The lowest energy configuration of  $\text{FePd}_{11}$  can be viewed as another cap on the  $\text{FePd}_{10}$  motif. The existence of a higher energy icosahedral



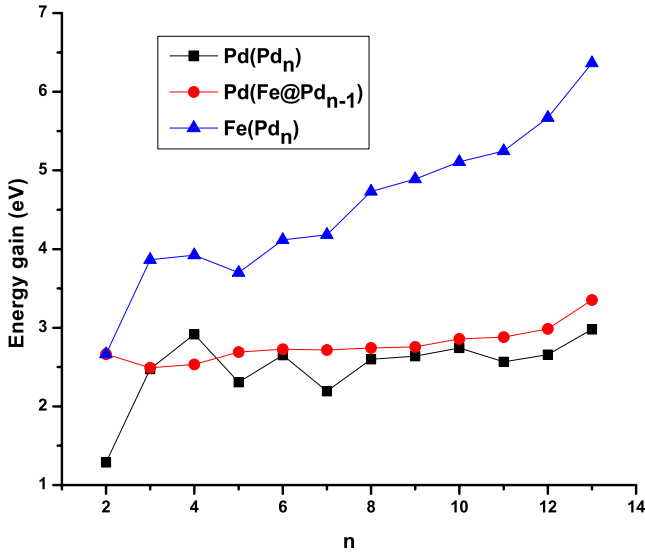
**Figure 3.** Binding energy per atom (eV/atom) of  $\text{Pd}_n$  and  $\text{FePd}_{n-1}$  ( $n = 2$ –13) clusters versus the number of atoms in the cluster.

$\text{FePd}_{11}$  structure with an Fe atom at the center, reveals the fact that as cluster size grows the Fe atom tries to move inwards to the host  $\text{Pd}_n$  cluster. The lowest energy structure of  $\text{FePd}_{12}$  is obtained by replacing the central Pd atom with an Fe atom on the icosahedral pure  $\text{Pd}_{13}$  cluster. Due to Fe doping the magnetic moment is enhanced to  $10 \mu_B$ , whereas the value is only  $8 \mu_B$  for the pure  $\text{Pd}_{13}$  cluster, and the binding energy increases to 2.57 eV/atom. In this structure the Fe–Pd distance is 2.6 Å and the separations between the Pd atoms forming the sphere vary from 2.7 to 2.8 Å.

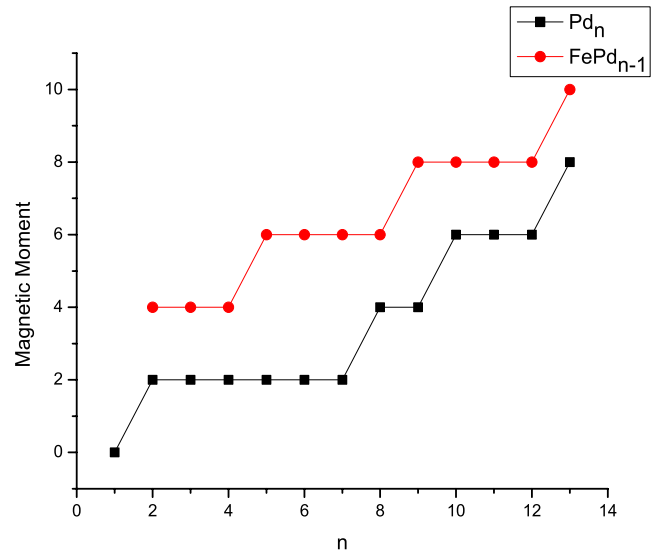
### 3.2. Electronic and magnetic properties

From the ground-state structures of the  $\text{FePd}_{n-1}$  cluster (section 3.1), our general observation is that the Fe atom in the lowest energy configuration tries to increase its coordination number by moving from the convex surface to the interior site, as the number of Pd atom varies from 2 to 12.

Figure 3 represents the comparison of binding energies for  $\text{Pd}_n$  and  $\text{FePd}_{n-1}$  clusters, both of which increase with  $n$ , as a result of the increase in the coordination number, and ultimately tend to saturate. In the  $\text{FePd}$  dimer, Mulliken population analysis shows that a small charge transfer (0.068) takes place from the Fe to the Pd site. A molecular orbital analysis shows that the Fe atom hybridizes with the Pd atom through the overlap of  $d_{z^2}$  orbitals. Thus, a partially covalent bond exists between the Fe and Pd atoms which is stronger than the Pd–Pd bonds. For all values of  $n$ , the BE of  $\text{FePd}_{n-1}$  cluster is consistently larger than the  $\text{Pd}_n$  cluster by a magnitude of 0.27–0.69 eV. This is due to the stronger Fe–Pd bond. To understand the systematic behavior of energy gains upon doping, we have calculated three different energetics, (a):  $E_1$ —the energy gain in adding a Pd atom to the  $\text{Pd}_n$  cluster, (b):  $E_2$ —the energy gain in adding a Pd atom to the  $\text{FePd}_{n-1}$  cluster and (c):  $E_3$  the energy gain in adding an Fe atom to the  $\text{Pd}_n$



**Figure 4.** The energy gain in adding an Fe and a Pd atom to Pd<sub>n</sub> and FePd<sub>n-1</sub> clusters. The squares ( $E_1$ ) and circles ( $E_2$ ) represent the energy gain in adding a Pd atom to Pd<sub>n</sub> and FePd<sub>n-1</sub> clusters respectively and the triangles represent ( $E_3$ ) the same for an Fe atom added to FePd<sub>n-1</sub> clusters.



**Figure 5.** The total magnetic moment (in  $\mu_B$ ) for the Pd<sub>n</sub> and FePd<sub>n-1</sub> structures as a function of the number of atoms in the cluster.

cluster. These are defined as follows:

$$E_1 = -[E(\text{Pd}_n) - E(\text{Pd}_{n-1}) - E(\text{Pd})] \quad (2)$$

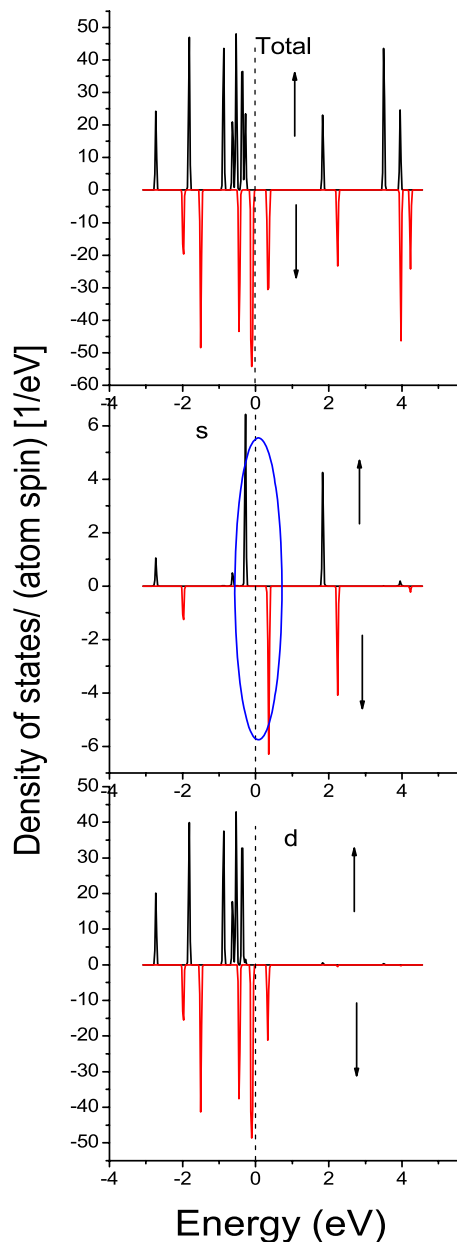
$$E_2 = -[E(\text{FePd}_n) - E(\text{FePd}_{n-1}) - E(\text{Pd})] \quad (3)$$

$$E_3 = -[E(\text{FePd}_n) - E(\text{Pd}_n) - E(\text{Fe})]. \quad (4)$$

Figure 4 shows the behavior of these energies as a function of size ( $n$ ). As noted in section 3.1, the Fe–Pd bond length is always shorter than Pd–Pd bond length. This observation along with figure 3 indicate that sp–d hybridization between the Pd atoms is weaker than the 3d–4d hybridization between the Fe and Pd atoms in the FePd<sub>n-1</sub> cluster. This can also be understood from figure 4, by noting that the energy gain in adding an Fe atom is always larger than that of adding a Pd atom to an existing pure Pd<sub>n</sub> cluster (i.e.  $E_3 \gg E_1$ ) and it always increases with cluster size (except  $n = 5, 7$ ). Similarly, the energy gain in adding a Pd atom to a Pd<sub>n</sub> cluster is always less than that in adding Pd to a FePd<sub>n-1</sub> cluster (i.e.  $E_1 < E_2$ ). The only exception is the pure Pd<sub>4</sub> cluster, which is presumably due to its extra stability. Figure 4 shows that as cluster size increases, the difference between  $E_3$  and  $E_1$  also increases (except for  $n = 4$ ). However, this difference ( $E_3 - E_1$ ) changes very rapidly (1.42 eV to 3.38 eV) when the cluster size grows from  $n = 6$  to 13, thus clearly indicating the preference for a higher coordination number of the Fe atom in the Pd host cluster. This is a direct reflection of the availability of the partially filled d-shells of Fe.

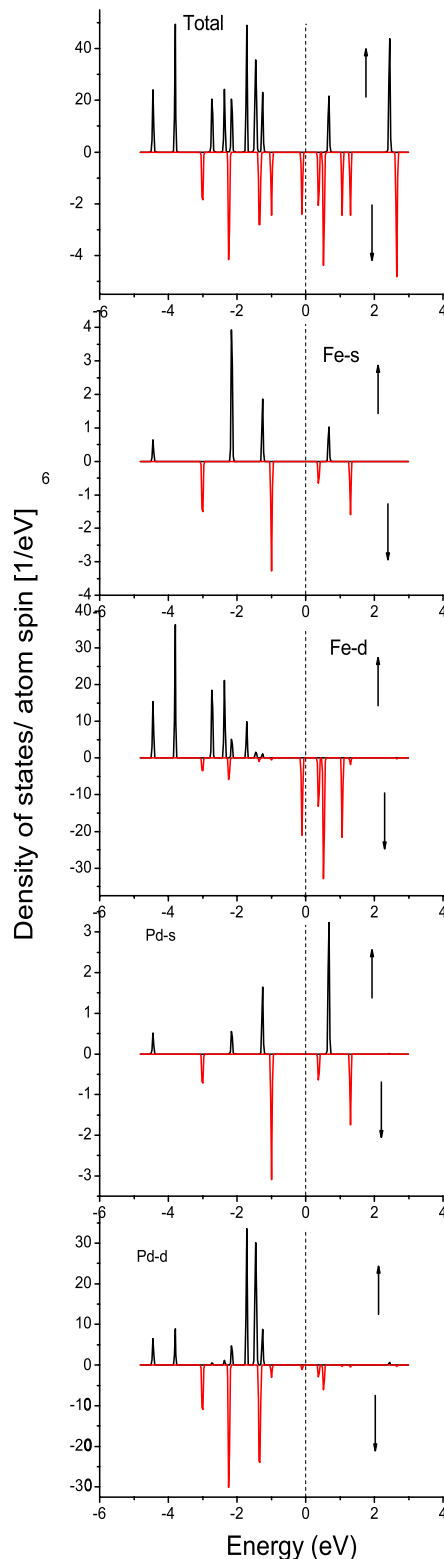
Now we examine the variation of the magnetic moment of FePd<sub>n-1</sub> clusters as a function of cluster size, as shown in figure 5, where we have also plotted the total moment of the Pd<sub>n</sub> clusters. The graph (figure 5) brings out three characteristic features. Firstly, there is an overall enhancement in the magnetic moment due to the doping of an Fe impurity in

the Pd matrix. Secondly, for both Pd<sub>n</sub> and FePd<sub>n-1</sub> clusters, a step function like behavior is observed in the total magnetic moment at some specific values of  $n$ . In pure Pd<sub>n</sub> clusters the jumps in magnetic moment occur at  $n = 2, 8$  and 10; whereas in the hetero-atomic FePd<sub>n-1</sub> clusters similar jumps occur at different  $n$ -values ( $n = 5, 9$  and 13). Thirdly, we find that, in the mid-size region ( $n = 5-7$ ), Fe substitution results in a three fold enhancement of the magnetic moment, which is remarkable. To understand the influence of the impurity atom in tailoring the magnetic property of the host cluster, the local magnetic moments at Fe and Pd sites are tabulated for comparison (table 1). The total magnetic moments of the pure and doped clusters are also listed in table 1. The local magnetic moment at each site can be calculated by integrating the difference of the spin-up and spin-down charge densities over a sphere of radius  $R$  centered on the site. For a particular cluster,  $R$  is so chosen such that no two spheres overlap i.e. the maximum value of  $R$  is equal to the half of the shortest bond length. For a given cluster size, the sum of local magnetic moment contributed from each site is less than the actual magnetic moment of the system, the difference being attributed to the interstitial contribution. It is observed (table 1) that, in the doped cluster the magnetic moment at the Fe impurity site remains more or less constant and the value (3.21–3.40  $\mu_B$ ) is close to the atomic moment (4.0  $\mu_B$ ) of Fe. It is to be noted that pure Pd<sub>n</sub> clusters are magnetic and their magnetic moments get enhanced with Fe doping. The step function like behavior of the graph (figure 5) comes from the variation of the local magnetic moment at Pd sites ( $\mu_B/\text{atom}$ ) (table 1). In order to substantiate the above discussions, we have analyzed the total and orbital decomposed densities of states (DOS). Firstly, we would like to examine the plots of the density of state of the pure Pd<sub>2</sub> dimer, shown in figure 6. The p-states are not shown due to their negligible contribution in the occupied region. It is to be noted that, the Pd atom is non-magnetic due to its closed shell electronic (4d<sup>10</sup>5s<sup>0</sup>) configuration. But when two



**Figure 6.** Gaussian broadened (width 0.02 eV) total and angular momentum decomposed density of states of the Pd<sub>2</sub> dimer. The vertical lines denote the HOMO level.

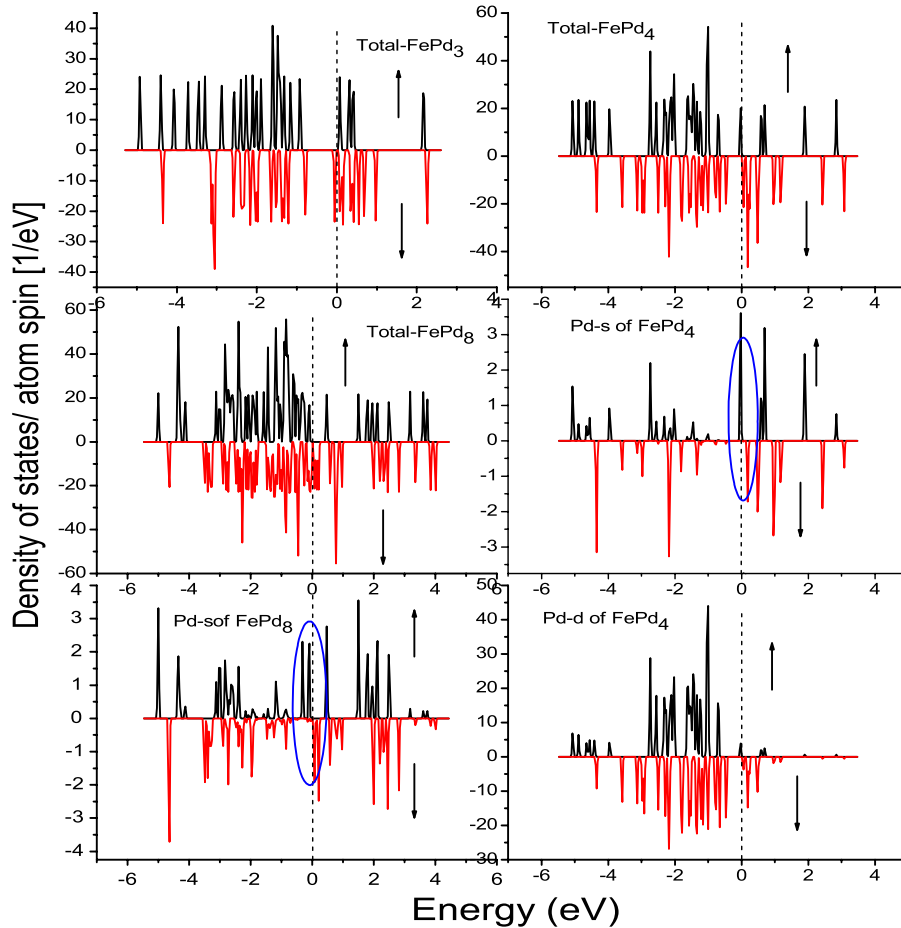
Pd atoms are brought together, s–d hybridization takes place and one electron from the down-spin d-state is promoted to the up-spin s-state. As a consequence, an occupied s level appears just below the HOMO level, while the corresponding down-spin d-state shifts just above the HOMO level, thus the Pd dimer acquires a  $2 \mu_B$  magnetic moment. A closer and systematic analysis of the density spectrum of the pure Pd<sub>n</sub> clusters (not shown) reveals that between the jumps, i.e. in the flat parts of the graph (figure 5), no further splitting in DOS occurs, and few unoccupied s levels begin to appear above the HOMO level. So in the flat regions (figure 5) ( $n = 2$ –7; 8–9; 10–12) the local magnetic moment per Pd atom decreases (except for Pd<sub>3</sub>) which is also reflected in table 1. In the case of Pd<sub>8</sub>, Pd<sub>10</sub> and Pd<sub>13</sub> structures, another additional spin splitting



**Figure 7.** Gaussian broadened (width 0.02 eV) total and angular momentum decomposed density of states of the FePd dimer. The vertical lines denote the HOMO level.

occurs that results into a jump in magnetic moment to the next higher values.

We now turn to the doped cluster. To understand the enhancement in the magnetic moment of FePd dimer, we



**Figure 8.** Gaussian broadened (width 0.02 eV) total and angular momentum decomposed density of states of FePd<sub>4</sub> and FePd<sub>8</sub> clusters. For comparison the total DOS of FePd<sub>3</sub> is also shown. The vertical lines denote the HOMO level.

**Table 1.** Magnetic moment.

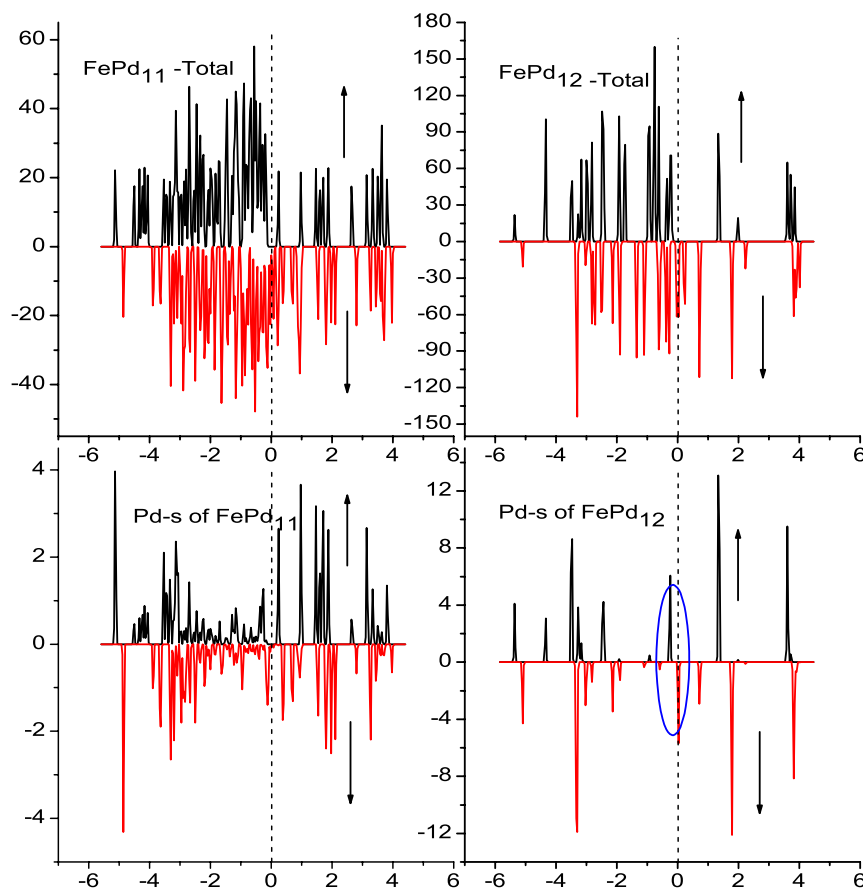
$n$	Pd <sub><math>n</math></sub> clusters		FePd <sub><math>n-1</math></sub> clusters		
	Total magnetic moment ( $\mu_B$ )	Local magnetic moment per Pd site ( $\mu_B/\text{atom}$ )	Total magnetic moment ( $\mu_B$ )	Local magnetic moment at Fe site ( $\mu_B$ )	Local magnetic moment per Pd site ( $\mu_B/\text{atom}$ )
2	2.0	0.61	4.0	3.37	0.43
3	2.0	0.63	4.0	3.26	0.29
4	2.0	0.48	4.0	3.21	0.23
5	2.0	0.39	6.0	3.45	0.45
6	2.0	0.33	6.0	3.44	0.36
7	2.0	0.28	6.0	3.43	0.38
8	4.0	0.45	6.0	3.41	0.31
9	4.0	0.40	8.0	3.61	0.44
10	6.0	0.52	8.0	3.38	0.43
11	6.0	0.49	8.0	3.40	0.39
12	6.0	0.47	8.0	3.31	0.38
13	8.0	0.53	10.0	3.34	0.49

analyze the total and s-, p- and d-projected DOS at the Fe and Pd sites which are shown in figure 7. The up-spin d-states at the Fe site are fully occupied while the electrons from the down-spin d-states are depleted and correspondingly few unoccupied states appear just above the HOMO level. Thus a magnetic moment of  $3.37 \mu_B$  close to its atomic moment value, is retained at the Fe site. Due to s-d hybridization, at the Pd site a few hybridized s and d levels appear just above the HOMO

level. This spin splitting induces a small moment ( $0.43 \mu_B$ ) at the Pd site.

As cluster size grows, successive addition of a Pd atom causes the total p-states contribution to increase. In FePd <sub>$n-1$</sub>  clusters, ( $n > 2$ ), Fe interacts with the host Pd atoms through s-d hybridization, whereas sp-d hybridization takes place between the Pd atoms. In the case of FePd<sub>2</sub> and FePd<sub>3</sub> clusters, a near constant moment value (table 1) is maintained at the





**Figure 9.** Gaussian broadened (width 0.02 eV) total and angular momentum decomposed density of states of FePd<sub>11</sub> and FePd<sub>12</sub> clusters. The vertical lines denote the HOMO level.

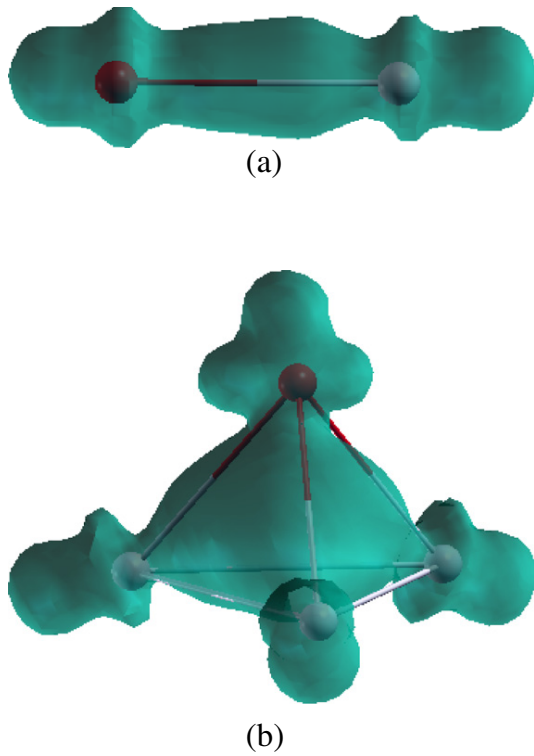
Fe site. The average moment at the Pd sites decreases (from 0.43 to 0.21  $\mu_B$ ), which retains the total magnetic moment of these clusters at 4  $\mu_B$ , and as a result there is no additional spin splitting.

As we move from the tetrahedral configuration of FePd<sub>3</sub> to the triangular FePd<sub>4</sub> configuration, the magnetic moment increases to 6  $\mu_B$ , which can be understood by analyzing the density of states of the FePd<sub>4</sub> cluster (figure 8) although the local magnetic moment at the Fe site increases slightly (3.21 to 3.45  $\mu_B$ ). It is clearly seen from figure 8 that in the FePd<sub>3</sub> cluster a few unoccupied states appear just above the HOMO level and one of these states becomes occupied in the FePd<sub>4</sub> cluster and drops below the HOMO level, resulting in an enhancement in the induced magnetic moment at the Pd sites of (0.45  $\mu_B$ /atom). The sp-d hybridization among Pd atoms is inferred from the s-, p- and d-projected DOS at the Pd sites (figure 8).

Further spin splitting is observed for the bi-capped PBP FePd<sub>8</sub> cluster, where the magnetic moment jumps to 8  $\mu_B$  due to the occurrence of a second hybridized level below the HOMO level (figure 8). For cluster sizes in the range  $n = 5-8$  and  $n = 9-12$ , the electrons get delocalized between the hybridized levels and total magnetic moments remain constant at 6  $\mu_B$  and 8  $\mu_B$  respectively.

The magnetic moment further increases to 10  $\mu_B$  in the case of the highly symmetric icosahedral FePd<sub>12</sub> cluster. This

is a typical example of a change in DOS (figure 9) because of a sudden change in geometry when the cluster acquires a high symmetry after the addition of one Pd atom in FePd<sub>11</sub>. The comparison between the DOS for cluster sizes with  $n = 12$  and 13 (figure 9) reveals that the spectrum of FePd<sub>12</sub> is gapped and eigenvalues show a degeneracy because of rotational symmetry. It can be seen that, as we move from FePd<sub>11</sub> to FePd<sub>12</sub>, the s-contributions at the Pd sites get enhanced by a factor of 4. The up-spin Pd s level, which now lies just above the HOMO level in the FePd<sub>11</sub> cluster, in case of FePd<sub>12</sub> cluster is pushed down just below the HOMO level and becomes occupied. However, except for being discrete the down-spin spectrum remains unchanged. Thus the induced magnetic moment at the Pd sites increases to its maximum of 0.49  $\mu_B$  and the magnetic moment of FePd<sub>12</sub> becomes 10  $\mu_B$  in totality. It is interesting to note that in this icosahedral structure the central Fe atom has 12 nearest neighbor Pd atom, thus it has the same chemical environment (at least up to first nearest neighbor) when Fe is introduced into a Pd fcc solid. In case of an Fe impurity in Pd bulk, the magnetic moment of Fe is 3.56  $\mu_B$ , while the induced moment on adjacent Pd atoms (12 nearest neighbors for the fcc lattice) is 6.91  $\mu_B$ , yielding a total magnetic moment of 10.47  $\mu_B$  [37]. In our present cluster calculation, FePd<sub>12</sub> corresponds to a symmetric icosahedral cluster with 12 nearest neighbor Pd atoms, the corresponding values of the local magnetic moments namely, 3.34  $\mu_B$  on



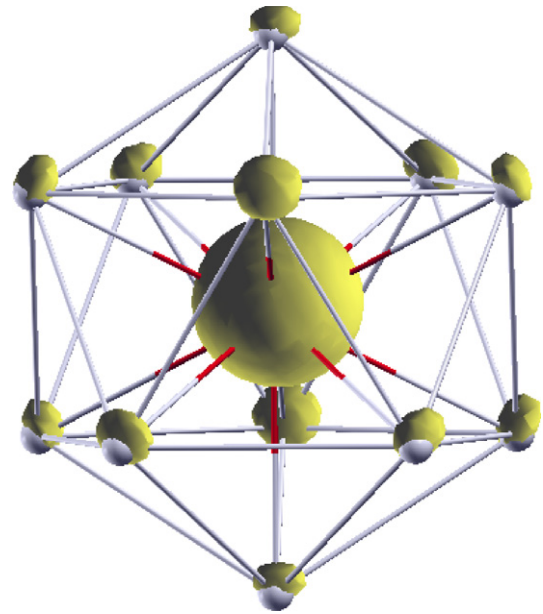
**Figure 10.** Isodensity surface corresponding to the HOMO-6 and HOMO-16 states for the lowest energy configuration of FePd (a) and FePd<sub>3</sub> (b) respectively, at one-fifth of its maximum isosurface value.

**Table 2.** HOMO–LUMO gap.

FePd <sub><i>n</i>-1</sub> cluster	HOMO–LUMO gap (eV)	
	Spin-up channel	Spin-down channel
2	1.92	0.48
3	1.49	0.33
4	1.04	0.18
5	0.62	0.53
6	0.58	0.35
7	0.63	0.25
8	0.40	0.13
9	0.57	0.11
10	0.57	0.09
11	0.44	0.20
12	0.43	0.09
13	1.56	0.19

Fe and 5.88  $\mu_B$  on Pd, agreeing with the corresponding bulk values.

For the doped cluster, it is interesting to study the variation of the HOMO–LUMO gap as a function of cluster size ( $n$ ). Calculated gaps both for upper and lower spin channels are listed in table 2. Irrespective of the cluster size the HOMO–LUMO gap for upper spin channel is always higher than those of lower spin channel. The up-spin HOMO–LUMO gap has its maximum value for the FePd dimer (1.92 eV). For cluster sizes with  $n = 5–12$ , due to an increase in coordination number the HOMO–LUMO gaps for the spin-up channel become less than



**Figure 11.** The spin density ( $\rho_\uparrow(r) - \rho_\downarrow(r)$ ) of the lowest energy configuration of FePd<sub>*n*-1</sub>, at one-fifteenth of its maximum isosurface value.

1 eV ( $\sim 0.40–0.63$  eV) and then suddenly increase to 1.56 eV for the case of the highly symmetric icosahedron FePd<sub>12</sub> configuration. However, the spin-down electrons have a very small gap (0.09–0.53 eV). Thus controlled electron transport can take place through the spin-down channel. Therefore Fe-doped palladium clusters could be considered as potential candidates in spintronics devices as spin analyzers or spin filters.

We have investigated the nature of bonding by examining the isodensity surface of the molecular orbital (MO). In our discussions to represent the typical occupied MO we are using the notation HOMO- $n$ , where  $n$  represents the number of levels between the highest molecular orbital (HOMO) to that of the occupied MO in the eigenvalue spectrum. Figure 10 shows the typical isodensity surface for HOMO- $n$  molecular orbital of the FePd and FePd<sub>3</sub> clusters. The eigenstate ( $n$ ) is chosen such that the corresponding MO shows the interaction among the Fe and surrounding Pd atoms, typically for most of the clusters we have found one such MO. The molecular orbitals, as shown in figure 10, clearly indicate the participation of a  $d_{z^2}$  orbital forming bond between the Fe and Pd atoms. In the case of the tetrahedral FePd<sub>3</sub> configuration, due to orbital overlap a uniform charge distribution is observed within the 3D cage, this makes the 3D configuration more stable.

It is interesting to examine the spin density isosurface of the ground-state configurations of the FePd<sub>(*n*-1)</sub> clusters. We consider a typical case of the highly symmetric icosahedral FePd<sub>12</sub> cluster whose spin density plot is shown in figure 11. It is observed that the majority of the magnetic moment is localized at the central Fe site and a small induced moment is found to be present at the Pd sites—a similar trend in spin density distribution is observed for all other cluster sizes.

#### 4. Conclusion

We have systematically investigated the structural, electronic and magnetic properties of pure and Fe-doped palladium clusters ( $\text{FePd}_{n-1}$ ,  $n = 2-13$ ) from first principles density functional theory. For each cluster size, an extensive search of the lowest energy structures has been conducted by considering a number of structural isomers. The overall evolutionary trends shows that, similar to pure  $\text{Pd}_n$ , the doped cluster follows the same icosahedral growth behavior where an Fe atom goes substitutionally in the host matrix. Single Fe doping in the  $\text{Pd}_{n-1}$  clusters enhances the BE of resultant  $\text{FePd}_{n-1}$  clusters. The subsequent larger energy gain in adding an Fe atom to a  $\text{Pd}_{n-1}$  cluster than that in adding a Pd atom ( $E_3 > E_1$ ) clearly indicates the preference for a higher coordination number for the Fe atom in the  $\text{FePd}_{n-1}$  cluster. In the doped cluster an enhancement in the magnetic moment is observed when the Fe impurity is substituted in the  $\text{Pd}_{n-1}$  cluster, however a three fold enhancement is observed in mid-sized ( $n = 5-7$ ) clusters. In the doped cluster the structural stability and magnetic properties appear to be a function of the coordination number of the Fe atom, the cluster symmetry and the sp-d hybridization among the Fe and Pd atoms. In the case of a highly symmetric icosahedral  $\text{FePd}_{12}$  cluster the central Fe atom gets 12 Pd atoms as nearest neighbors and consequently the magnetic moment increases to  $10 \mu_B$ , thus reproducing the magnetic behavior when Fe is introduced into a Pd-solid. Thus it is only the nearest neighbor Pd atoms that get the induced magnetic moments, thereby reiterating our conjecture that this enhancement of magnetism is a 'local' phenomena. It should be pointed out here that in the present calculation collinear alignment of spins are only taken into account and the effect of non-collinear spins is considered to be insignificant as far as energetics is concerned.

#### Acknowledgments

GPD would like to thank Professor S N Mishra and Dr M S Bahramy for many helpful discussions.

#### References

- [1] Jellinek J and Krissinel E B 1999 *Theory of Atomic and Molecular Clusters* ed J Jellinek (Berlin: Springer) pp 277-308
- [2] Bloomfield L A, Deng J, Zhang H and Emmert J W 2000 *Proc. Int. Symp. Cluster and Nanostructure Interface* ed P Jena, S N Khanna and B K Rao (Singapore: World Scientific) p 131
- [3] Klabunde K J 1994 *Free Atoms, Clusters, and Nanoscale Particles* (New York: Academic)
- [4] Klabunde K J 2001 *Nanoscale Materials in Chemistry* (New York: Wiley)
- [5] Kumar V, Esfarjani K and Kawazoe Y 2002 *Clusters and Nanomaterials (Springer Series in Cluster Physics)* ed Y Kawazoe and K Ohno (Heidelberg: Springer) p 9
- [6] Kondov T and Maufune F (ed) 2003 *Progress in Experimental and Theoretical Studies of Clusters* (New York: World Scientific)
- [7] Seifert G 2004 *Nat. Mater.* **3** 77
- [8] Kumar V and Kawazoe Y 2001 *Phys. Rev. Lett.* **87** 045503
- [9] Khanna S N and Jena P 1992 *Phys. Rev. Lett.* **69** 1664
- [10] Rao B K, Jena P, Manninen M and Neiminen R M 1987 *Phys. Rev. Lett.* **58** 1188
- [11] Bilas I M L, Chatelain A and de Heer W A 1994 *Science* **265** 1682
- [12] Cox A J, Louderback J G and Bloomfield L A 1993 *Phys. Rev. Lett.* **71** 923
- [13] Cox A J, Louderback J G, Apsel S E and Bloomfield L A 1994 *Phys. Rev. B* **49** 12295
- [14] Douglass D C, Bucher J P and Bloomfield L A 1992 *Phys. Rev. B* **45** 6341
- [15] Ganteför G and Eberhardt W 1996 *Phys. Rev. Lett.* **76** 4975
- [16] Taniyama T, Ohta E and Sato T 1997 *Europhys. Lett.* **38** 195
- [17] Moseler M, Häkkinen H, Barnett R N and Landman U 2001 *Phys. Rev. Lett.* **86** 2545
- [18] Kumar V and Kawazoe Y 2002 *Phys. Rev. B* **66** 144413
- [19] Lee K 1991 *Phys. Rev. B* **58** 2391
- [20] Moruzzi V L and Marcus P M 1989 *Phys. Rev. B* **39** 471
- [21] Fritsche L, Noffke J and Eckardt H 1987 *J. Phys. F: Met. Phys.* **17** 953
- [22] Chen H, Brener N E and Callaway J 1989 *Phys. Rev. B* **40** 1443
- [23] Oswald A, Zeller R and Dederichs P H 1986 *Phys. Rev. Lett.* **56** 1419
- [24] Low G G and Holden T M 1966 *Proc. Phys. Soc. Lond.* **89** 119
- [25] Clogston A M, Matthias B T, Peter M, Williams H J, Corenzwit E and Sherwood R C 1962 *Phys. Rev.* **125** 541
- [26] Schroeder P A and Uher C 1978 *Phys. Rev. B* **18** 3884 and references therein
- [27] van Acker J F, Weijs P J W, Fuggle J C, Horn K, Haak H and Buschow K H J 1991 *Phys. Rev. B* **43** 8903 and references therein
- [28] Verbeek B H, Nieuwenhuys G J, Mydosh J A, van Dijk C and Rainford B D 1980 *Phys. Rev. B* **22** 5426
- [29] Rader O, Carbone C, Clemens W, Vescovo E, Bligel S, Eberhardt W and Gudat W 1992 *Phys. Rev. B* **45** 13823
- [30] Celinski Z, Heinrich B, Cochran J F, Muir W B, Arrott A S and Kirschner J 1990 *Phys. Rev. Lett.* **65** 1156
- [31] Lee S K, Kim J S, Kim B, Cha Y, Han W K, Min H G, Seo J and Hong S C 2001 *Phys. Rev. B* **65** 014423
- [32] Rader O, Vescovo E, Redinger J, Blugel S, Carbone C, Eberhardt W and Gudat W 1994 *Phys. Rev. Lett.* **72** 2247
- [33] Cheng L, Altounian Z, Ryan D H, Strom-Olsen J O, Sutton M and Tun Z 2004 *Phys. Rev. B* **69** 144403
- [34] Yiping L, Hadjipanayis G C, Sorensen C M and Klabunde K J 1994 *J. Appl. Phys.* **75** 5885
- [35] Sato K, Bian B and Hirotsu Y 2002 *J. Appl. Phys.* **91** 8516
- [36] Taniyama T, Ohta E, Sato T and Takeda M 1997 *Phys. Rev. B* **55** 977
- [37] Guzman M, Delplancke J L, Long G J, Delwiche J, Hubin-Franskin M-J and Grandjean F 2002 *J. Appl. Phys.* **92** 2634
- [38] Wunder R and Phillips J 1994 *J. Phys. Chem.* **98** 12329
- [39] Guirado-López R A, Desjonquères M C and Spanjaard D 2006 *Phys. Rev. B* **74** 064415
- [40] Delley B, Ellis D E and Freeman A J 1982 *J. Magn. Magn. Mater.* **30** 71
- [41] Sun Q, Wang Q, Yu J Z, Li Z Q, Wang J T and Kawazoe Y 1997 *J. Physique I* **7** 1233
- [42] Nigam S, Majumder C and Kulshreshtha S K 2007 *Phys. Rev. B* **76** 195430
- [43] Srivastava S K, Mishra S N and Das G P 2006 *J. Phys.: Condens. Matter* **18** 9463
- [44] Bahramy M S, Srivastava S K, Mishra S N, Das G P and Kawazoe Y 2007 *J. Magn. Magn. Mater.* **310** e541
- [45] Blöchl P E 1994 *Phys. Rev. B* **50** 17953
- [46] Kresse G and Joubert D 1999 *Phys. Rev. B* **59** 1758
- [47] Perdew J P, Burke K and Ernzerhof M 1996 *Phys. Rev. Lett.* **77** 3865
- [48] Furthmüller G 1996 *Phys. Rev. B* **54** 11169